Numerical Simulations of the Meteorological and Dispersion Conditions during an Air Pollution Episode over Athens, Greece

V. KOTRONI, G. KALLOS, K. LAGOUVARDOS, AND M. VARINOU

Laboratory of Meteorology, Department of Applied Physics, University of Athens, Athens, Greece

R. WALKO

Department of Atmospheric Sciences, Colorado State University, Fort Collins, Colorado

(Manuscript received 30 June 1997, in final form 3 March 1998)

ABSTRACT

In this study a summer air pollution episode from 6 to 8 August 1994 over Athens, Greece, is investigated through advanced atmospheric modeling. This episode was reported from the air quality monitoring network, as well as from research aircraft measurements performed during this period for the Transport and Transformation of Air Pollutants from Europe to the East Mediterranean region project. The meteorological conditions prevailing during the period 6–8 July 1994 are analyzed based on simulations performed with the Colorado State University–Regional Atmospheric Modeling System and on the available surface and upper-air observations. Indeed, the synoptic settings induced favorable conditions for the development of local-scale circulations, which defined the poor dispersion conditions over the area. The dispersion of the urban plume of Athens is studied with the use of the Hybrid Particle and Concentration Transport package model. The urban plume of Athens is tracked down the Saronic Gulf and the eastern coast of Peloponnisos, more than 200 km southward from the Athens Basin in good agreement with the research aircraft observations.

1. Introduction

During the last 20 years the air quality problem has been considered over the greater Athens area (GAA) from the combination of high air pollutant emissions and the complex character of the boundary layer dynamics over the area. The largest part of the air pollutant emissions is attributed to automobiles, industry, and central heating during the cold months. It is worth mentioning that one-third of the Greek population resides in the GAA. The pollutant transport and transformation conditions within the GAA are defined from the interaction of synoptic, regional, meso- and microscales. Under weak synoptic forcing, thermally driven circulations develop to create poor dispersion conditions within the GAA (Kallos et al. 1993; Pilinis et al. 1993; Kassomenos et al. 1995).

Several observational and modeling exercises have been conducted in the past with the aim of contributing to air pollution abatement strategies over the GAA. Most of the field campaigns focused on the analysis of the photochemical pollution, the vertical distribution of ozone, and nighttime pollutant transport in connection with the sea-breeze circulation (Lalas et al. 1982; Lalas et al. 1983; Lalas et al. 1987; Asimakopoulos et al. 1992). These campaigns provided evidence of the recirculation of air pollutants and the cumulative effect created by the land–sea-breeze diurnal cycle. Most of the model investigators who studied air quality in Athens agreed that it is fundamental for an optimized air pollution control strategy to accurately define the atmospheric circulations (Kunz and Moussiopoulos 1995), as the effect of wind field specification can have a greater impact on the results of photochemical models and prognosed concentrations than the chemical mechanisms employed in these models (Giovannoni and Russell 1995). Most of the aforementioned studies were focused on the GAA where the density of the emissions under certain meteorological conditions can lead to considerable concentrations downwind to rural areas.

During the period 1993–95 the European Union–financed Transport and Transformation of Air Pollutants for Europe to the East Mediterranean region project (T-TRAPEM) was carried out, which, among others, aimed at tracking the urban plume of Athens through observational and modeling analyses (Kallos et al. 1996). On 6–8 July 1994 an air pollution episode occurred in the GAA. Indeed, O_3 concentrations exceeded the ‘‘alert

Corresponding author address: V. Kotroni, Laboratory of Meteorology, Dept. of Applied Physics, University of Athens, Panepistimioupolis, Bldg. PHYS-V, 15784 Athens, Greece.
E-mail: kotroni@etesian.dap.uoa.gr

standards'' of 100 ppbv at the least at two stations (four stations on 7 July) of the monitoring network in the GAA, for a period greater than 2 h per day (Peleg et al. 1997). Due to the reported concentrations on 7 and 8 July restrictions have been imposed on industrial emissions and traffic of civilian cars in the GAA. During this period a research aircraft measurement campaign was performed providing air pollutant measurements over the GAA, the Saronic Gulf, and the eastern border of Peloponnisos, where the measured pollutant concentrations were well above the background level not only over Athens but also farther away near the eastern border of Peloponnisos. Indeed, while background concentrations in the vicinity of the GAA for the summer range between 40 and 60 ppbv, during the period 6–8 July concentrations greater than 120 and 80 ppbv have been reported over the GAA and the maritime area of Peloponnisos, respectively (Peleg et al. 1997). These observations incited the extensive modeling study of the meteorological conditions leading to this episode. The model used is the Colorado State University–Regional Atmospheric Modeling System (CSU–RAMS), which permitted the study of the interaction of the different scales of motion in defining the regional- and local-scale flow through its nesting capabilities. Model results are also evaluated through analysis of the available meteorological data. The behavior of the urban plume under the prevailing meteorological conditions is studied through the use of the modeling system Hybrid Particle and Concentration Transport Package (HYPACT), which is driven by the RAMS meteorological fields.

Section 2 describes the meteorological conditions prevailing during the case study. In section 3 the modeling system used is presented, while the model results (meteorological and dispersion) are presented and compared to the observations in section 4. The last section discusses the results.

2. Meteorological conditions

From 5 to 8 July 1994, the Mediterranean region was characterized by stationary conditions devoid of significant weather events, with a high pressure system established over the Balkans and the greatest part of the Mediterranean region. Over the Dardanelles the pressure gradient was weak, giving rise to a weak northerly flow. The high pressure system dominating the greatest part of the Mediterranean region at 1200 UTC 6 July 1994 extends eastward over western Turkey, limiting the extension of the southwestern Asia thermal low over central Turkey (Fig. 1a). These synoptic settings result in a light northerly flow at the surface as well as aloft over the Aegean Sea and allow the development of mesoscale thermal circulations in the area of interest. These local-scale circulations influence the transport and dispersion of air pollutants over the GAA, forming, in general, poor dispersion conditions in the Attica Peninsula and Saronic Gulf. Weak dispersion conditions are also created when a warming at the lower-tropospheric layers occurs. Figures 1b and 1c show the 850-hPa temperature field at 1200 UTC 6 and 7 July 1994 constructed from the European Centre for Medium-Range Weather Forecasts (ECMWF) gridded data (horizontal analysis of $1° \times 1°$). During this 24-h elapsed time, a warming is evident over the entire Greek peninsula due to warm-air advection from the southwest. Kallos et al. (1993) concluded that the most favorable conditions for air pollution episodes is when the synoptic flow is weak, favoring the development of local thermal circulations, and/or there is warm advection in the lower troposphere, which is exactly the case on the reported period.

Inspection of the soundings performed at the Athens airport (collocated with GMS station shown in Fig. 4) at 0000 and 1200 UTC from 5 to 7 July 1994 (Fig. 2) shows the following. At 1200 UTC there is an average warming of 2 K aloft from the 750- to 500-hPa level from 5 to 6 July, while during the following 24 h there is a warming of about 2.5 K at the lower tropospheric layers (from the surface to 750 hPa). At 0000 UTC, a successive warming occurs from the surface to about 700 hPa at a rate of 2 K per 24 h. It is worth noting that at 0000 UTC 7 July, the day that the air pollution episode occurred, there was a surface inversion of about 5° over a layer of 500 m. A temperature inversion climatology performed by Kassomenos et al. (1995) for the period 1983–1990 showed that nocturnal surface inversions occurred for 95% of the nights of ''air pollution episode days.''

The development of sea breezes from the meteorological surface network recordings in the GAA is presented in Fig. 3 (for the stations' locations, see Fig. 4). Indeed, on 6 July calm or light winds are reported in the early morning, followed later by a sea breeze that develops and penetrates farther inland, and ultimately reaches the TAT station near the foothills in the late afternoon. On 7 July the sea breeze is evident only on the coastal stations (GMS, ELE) and reaches the basin at 1500 UTC (NOA and NFL stations). On 8 July the sea breeze is observed only at the coastal stations of GMS and ELE and does not seem to penetrate into the basin. The sea-breeze development and inland penetration will be further investigated and discussed in section 4, based on the model results. Sea-breeze characteristics in the Attica Peninsula have been extensively analyzed in the past, based on analyses of observations (Prezerakos 1986; Lalas et al. 1983; Lalas et al. 1987; Asimakopoulos et al. 1993; Kallos et al. 1993; Helmis et al. 1995) and analyses of model results (Steyn and Kallos 1992; Varvayanni et al. 1993; Kunz and Moussiopoulos 1995; Melas et al. 1995), due to their important role on the definition of the local climatic characteristics and on their contribution to increased levels of photochemical pollution.

The aforementioned meteorological conditions contributed to an air pollution episode over the GAA. Indeed, on 6, 7, and 8 July the ozone levels exceeded 100 ppbv with peaks of 120 ppbv (mainly on 7 and 8 July) at several stations of the air quality monitoring network.

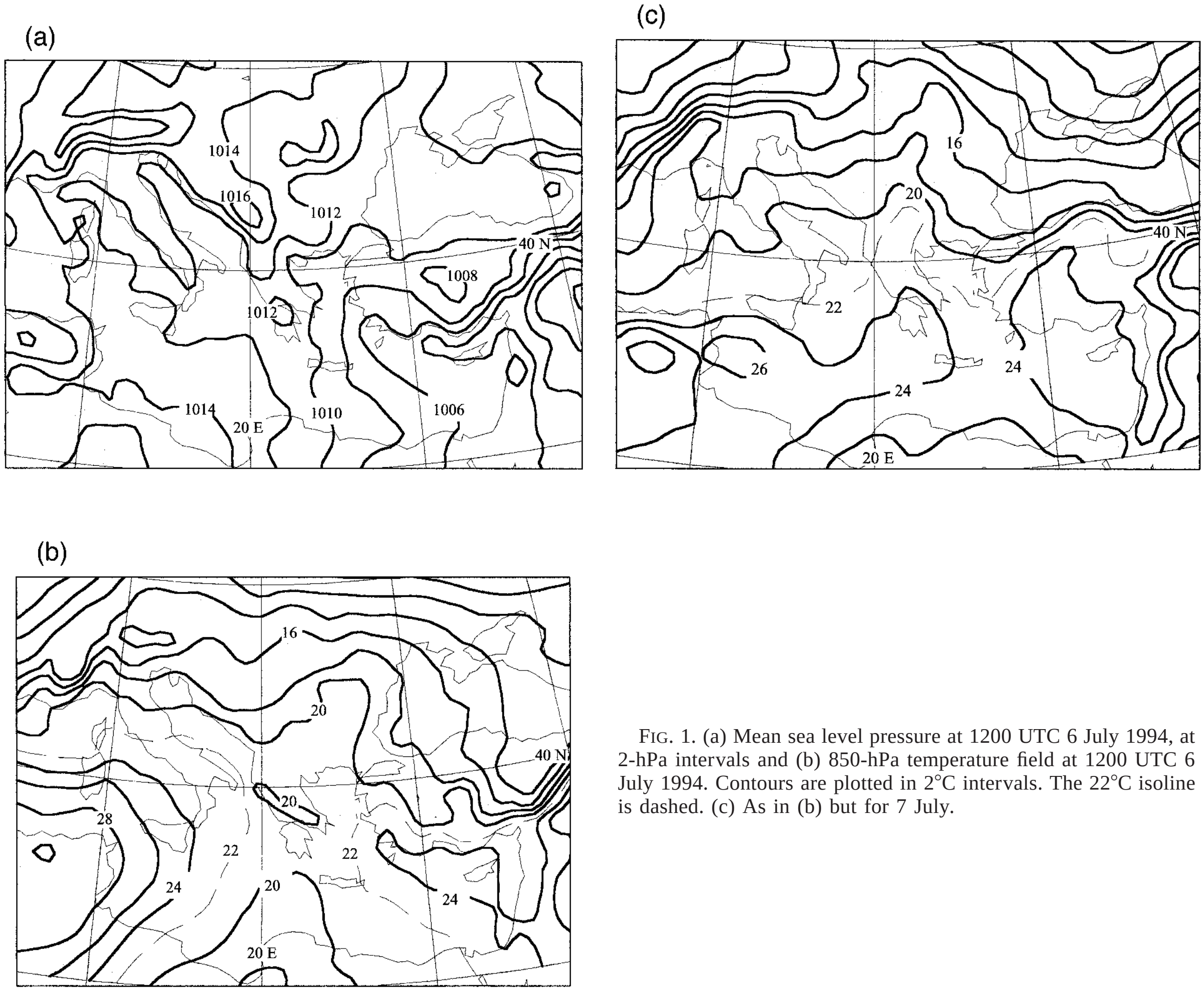

FIG. 1. (a) Mean sea level pressure at 1200 UTC 6 July 1994, at 2-hPa intervals and (b) 850-hPa temperature field at 1200 UTC 6 July 1994. Contours are plotted in 2°C intervals. The 22°C isoline is dashed. (c) As in (b) but for 7 July.

High ozone concentrations have also been reported from the research aircraft flights, not only over the GAA but also over the Saronic Gulf and the eastern coast of Peloponninos, implying that the urban plume of Athens also affects remote areas. Detailed description of the air quality during this event from both the monitoring network observations and research flight data is given in Peleg et al. (1997). In the present work, this air pollution episode will be further investigated and discussed through modeling exercises, including atmospheric model simulations, in order to study the prevailing meteorological conditions and Lagrangian particle dispersion modeling, which will assist in analyzing the transport mechanisms of the Athens urban plume.

3. Description of the modeling system

a. The RAMS model

RAMS was developed at Colorado State University and the ASTER Division of the Mission Research Corporation (Pielke et al. 1992). RAMS uses the full set of primitive dynamical equations with optional parameterization schemes for turbulent diffusion; solar and terrestrial radiation; and sensible and latent heat exchange between the atmosphere, multiple soil layers, the kinematic effects of terrain, and a vegetation canopy.

An important feature of RAMS is its capacity to perform two-way interactive grid nesting, which allows local fine-mesh grids to resolve small atmospheric systems, while simultaneously modeling the large-scale environment of the systems on a coarser grid. The most important features of RAMS are summarized in Pielke et al. (1992). Specific applications of this modeling system to air quality studies are reviewed in Pielke et al. (1991) and Lyons et al. (1993). Recent air quality studies based on the application of RAMS can be found in Fast et al. (1995), Poulos and Bossert (1995), Lyons et al. (1995) Lagouvardos et al. (1996), and Bossert (1997).

b. The HYPACT model

HYPACT was developed at the Colorado State University and the ASTER Division of the Mission Re-

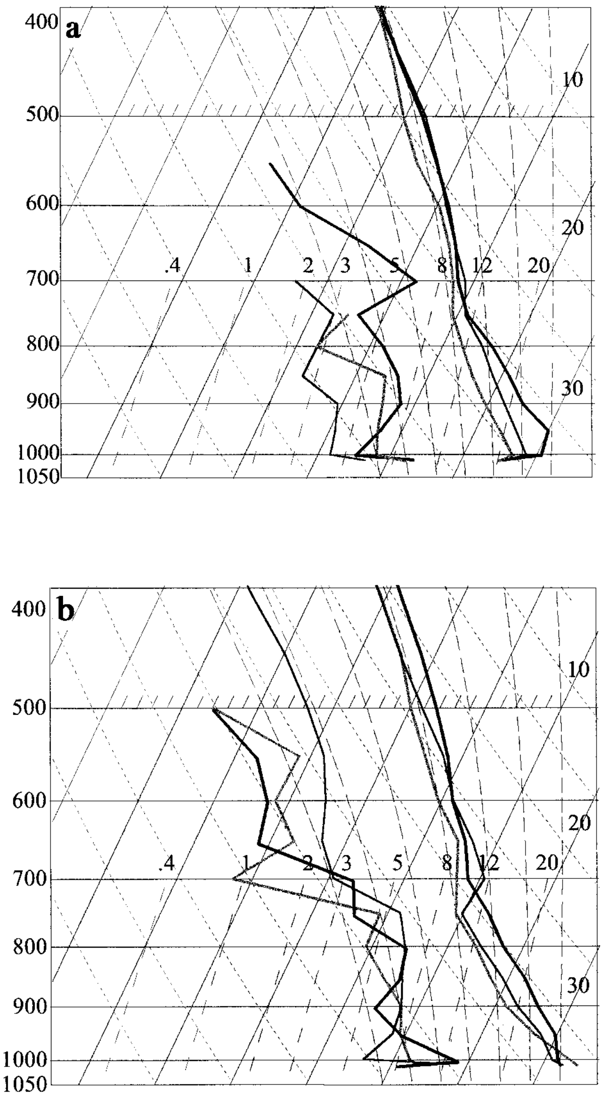

FIG. 2. Upper-air sounding at (a) 0000 and (b) 1200 UTC, 5 (gray line), 6 (thin line), and 7 (bold line) July 1994.

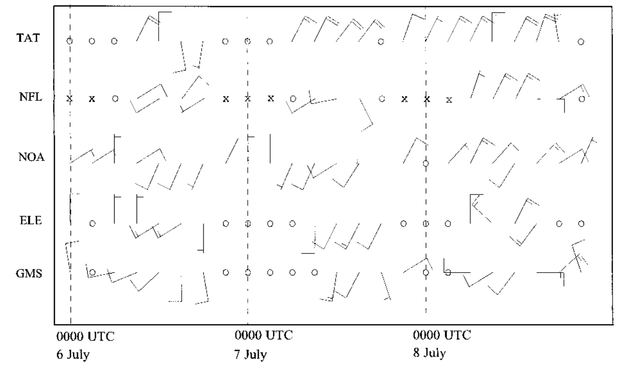

FIG. 3. Winds at the anemometric level reported from the meteorological surface network at 3-h intervals. The location of the surface stations is reported in Fig. 4b. Open circles denote calm, while ×'s denote missing data. One barb equals 4 m s^{-1}, one-half barb equals 2 m s^{-1}.

search Corporation (Tremback et al. 1994). It is a combination of a Lagrangian particle model and a Eulerian concentration transport model. With the Lagrangian part of the model, the particles are advected with mean and random turbulent wind components using the velocity and turbulence fields simulated by RAMS. The source configurations of HYPACT are very flexible. Any number of sources can be specified anywhere in the domain and configured as a point, line, area, or volume source, while these sources can be instantaneous, intermittent, or continuous. A recent application of the combined RAMS and HYPACT model can be found in Lyons et al. (1994) and Lagouvardos et al. (1996).

c. Model setup

The presence of a complex shoreline and the pronounced terrain irregularities, not only of the GAA but

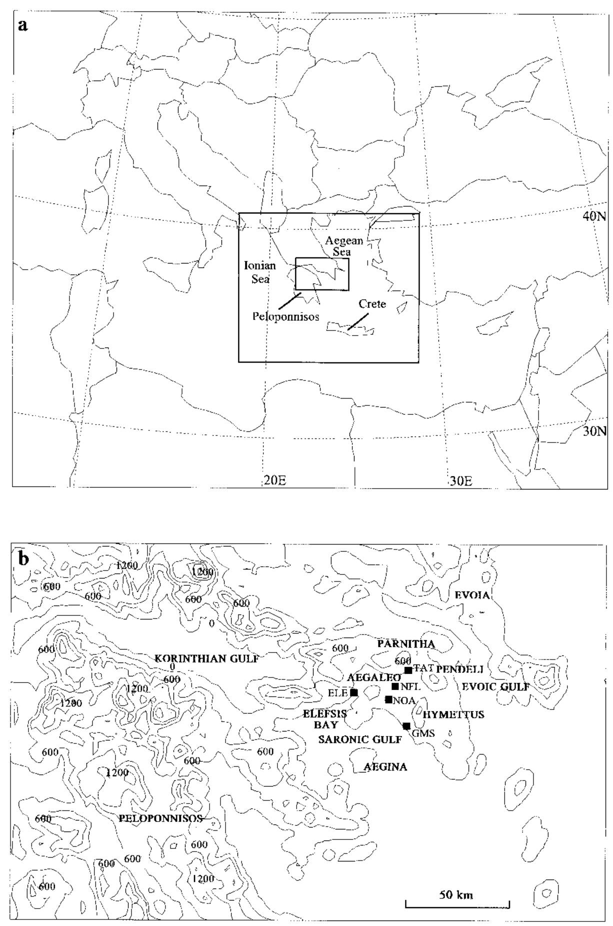

FIG. 4. (a) Domain of the three nested grids used for the simulations and (b) map of the GAA. Elevations are every 300 m. Squares indicate the location of the meteorological surface stations.

also of the entire Greek peninsula, play a significant role on the diurnal variation of the thermally forced circulations and as a matter of fact on the definition of the local flow characteristics. The effects of the selected domain in mesoscale atmospheric simulations and dispersion calculations over the GAA have been discussed in Kallos and Kassomenos (1994), in which the authors argued that an inaccurate definition of the grids may result in the failure of reproduction of the local thermal circulations. Thus special care has been taken for the definition of the model domain and especially for the definition of the finer grid, which will allow the local-scale flow pattern to be resolved. For the present study a three-nest model domain has been defined.

1) The outer model domain has a horizontal grid increment of 32 km with 100 × 80 grid points centered at 39.000°N, 22.500°E.
2) The second model domain has horizontal grid increment of 8 km with 122 × 102 grid points centered at 37.128°N, 23.596°E.
3) The fine model domain has a horizontal grid increment of 2 km with 142 × 90 grid points centered at 37.849°N, 23.190°E.

Twenty-two vertical levels following the topography were used in all grids beginning with 180-m vertical spacing near the ground, increasing to 1 km at an altitude of 6 km, and remaining constant up to about 16 km. The model domain and relative location of each grid are given in Fig. 4a. The inner grid (Fig. 4b) has been defined so as to include, in addition to the greater Athens area, the island of Evvoia on the east, the Gulf of Corinth on the west, and the eastern coast of Peloponnisos. This extended finer grid made the simulation computer expensive, but it was considered to be necessary in order to accurately simulate the atmospheric flow over such a complex terrain. As seen in Fig. 4b, the GAA is surrounded by mountains on the three sides with a major opening to the sea in the southwest. More precisely Mount Aegaleo is located to the west of the basin, Parnitha to the north-northwest, Pendeli to the north-northeast, and Hymettus to the east. These mountains act like physical barriers on the flow with only small gaps between them; the flow is also modified by the hills up to 200 m located inside the basin (Pnyka, Lycabettus, and Tourkovounia). Note that the Gulf of Corinth is surrounded by high mountains both to the north and to the south, which results in a channeling of the flow.

The simulation started at 0000 UTC 6 July 1994 and ended 72 h later. The ECMWF 1° gridded analysis files (including geopotential height, horizontal wind components, temperature, and relative humidity at 11 pressure levels—the 925-hPa level included) were used to initialize the model. The ECMWF data are objectively analyzed by the RAMS model on isentropic surfaces from which they are interpolated to the RAMS grids. These fields were used to nudge the lateral boundary region of the coarser grid every hour. The ECMWF fields of the climatological sea surface temperature (1° resolution) and topography derived from 30-s terrain data retrieved from the National Center for Atmospheric Research (NCAR) have been used for all grids. Moreover, vegetation-type data with 10-min horizontal resolution were used.

To study the dispersion of the urban plume of Athens, the Lagrangian option of HYPACT has been used. Hourly output from RAMS is used as input for HYPACT. For the Lagrangian simulations the Athens urban area has been defined as an area source with a horizontal extension of 10 km × 10 km. Further details for the Lagrangian particle simulations will be given in section 4.

4. Model results

a. Meteorological results

At 0600 UTC 6 July 1994, a weak northeasterly flow is evident over the exit of Dardanelles (Fig. 5a), which backs to the northern and northwestern directions and intensifies in the central part and then at the exit of the Aegean Sea (east of Crete). Over the Ionian Sea, the near-surface flow is westerly and then northwesterly in the area west and south of Peloponnisos. Over the Saronic Gulf, northerly winds of the order of 2–4 m s^{-1} prevail, while in the Athens Basin the flow is weak with variable direction (Fig. 6a).

Due to the weak synoptic flow, local thermal circulations begin to develop later in the day. Sea-breeze circulations over the Attica Peninsula have been studied in the past based on climatological (Prezerakos 1986) or observational (Lalas et al. 1983; Asimakopoulos et al. 1993; Helmis et al. 1987; Helmis et al. 1995) methods, as well as modeling (Steyn and Kallos 1992; Varvayanni et al. 1993, Kunz and Moussiopoulos 1995; Melas et al. 1995). These studies revealed that the sea-breeze activity manifests itself through the development of three separate inland propagating systems: from Elefsis Bay in the southwest, from Saronic Gulf in the south, and from the Gulf of Evvoia in the east. At 0900 UTC 6 July 1994 the sea-breeze cell from Elefsis Bay is evident, with a vertical extent to 400 m, while soon after the two other cells develop (not shown).

At this point one should mention that there is a mesoscale flow that develops around Peloponnisos and strongly interacts with the sea-breeze cells over the Attica Peninsula. More specifically, at 1200 UTC 6 July (Fig. 5b), the westerly-northwesterly flow depicted west of Peloponnisos diverges south to a southern flow that reaches the Attica Peninsula and to a northwesterly flow directed toward Crete. Compared to the synoptic network recordings, the predicted flow reproduces the weak flow over the northern Aegean Sea and northern Greece, which intensifies at the exit of the Aegean Sea (east of Crete), the northwesterly flow over Crete, and the sea-breeze flow over the Attica Peninsula. Surface network wind reports are used to validate the model-predicted

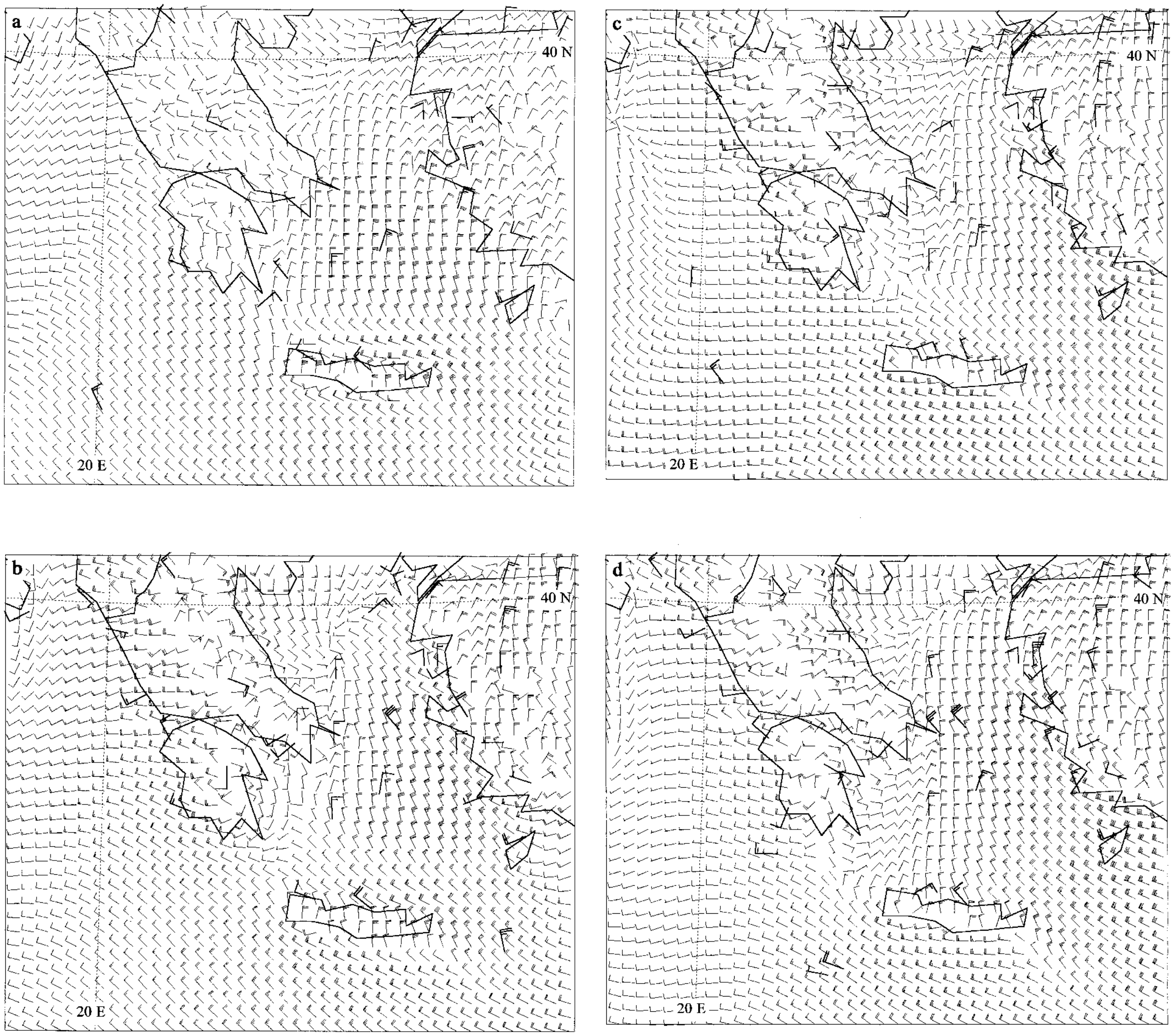

FIG. 5. Winds at $z = 86$ AGL from the second grid of RAMS at (a) 0600 UTC 6 July, (b) 1200 UTC 6 July, (c) 1200 UTC 7 July, and (d) 1200 UTC 8 July 1994. Barbs are plotted every third grid point. One barb equals 4 m s^{-1}, one-half barb equals 2 m s^{-1}. Large barbs denote surface winds reported from the synoptic network.

winds; however, one should note at this point that some differences between the observed and predicted winds can be attributed to the fact that the surface network reports winds at the anemometric level, that is, at 10 m above ground level (AGL), while the first near-surface model level of RAMS is at $z = 85$ m AGL. The aforementioned type of divergent flow has been also discussed in Kallos et al. (1993). This mesoscale flow interacts with the sea-breeze cells as follows. It adds up and reinforces the southerly winds of the Saronic Gulf sea breeze, while the interaction with the Evvoic Gulf sea-breeze cell results in the weakening and suppression of this cell (the latter is evident for the hours shown in Fig. 6c). Indeed, at 1200 UTC 6 July, the wind field from the inner grid of RAMS shows that the sea-breeze cells of the Saronic Gulf and Elefsis have penetrated inland (Fig. 6b).

Figure 6c depicts the near-surface flow from the inner grid of RAMS at 1500 UTC, where the reinforced southern flow from the Saronic Gulf as well as the suppression of the Evvoic Gulf cell are evident. This flow reached the foothills of Parnitha (predicted wind speed of the order of 5 m s^{-1}), where the surface station TAT reported southern winds of the order of 4 m s^{-1} (Fig. 3). The aforementioned mesoscale flow is evident until 1800 UTC.

During the nighttime hours of 7 July, the wind flow over the basin is weak (2–3 m s^{-1}) from variable directions. The wind flow is also weak over the Saronic Gulf and the Aegean Sea, while it is somehow more

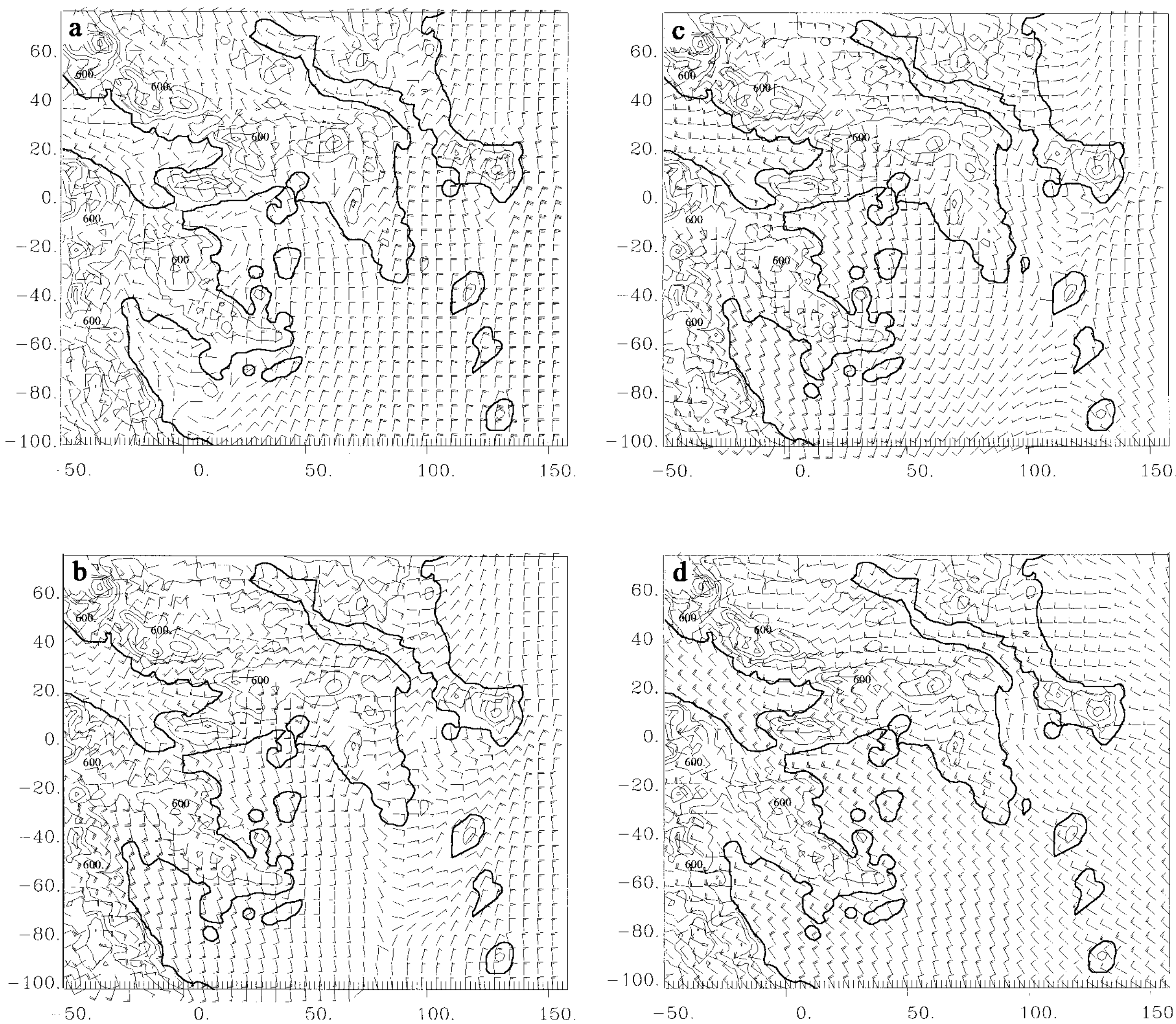

FIG. 6. Winds at z = 86 AGL from the inner grid of RAMS at (a) 0600 UTC 6 July, (b) 1200 UTC 6 July, (c) 1500 6 July, (d) 0000 7 July, (e) 1200 UTC 7 July, and (f) 1200 UTC 8 July 1994. Barbs are plotted every third grid point. One barb equals 4 m s^{-1}, one-half barb

intensified over the Gulf of Corinth (Fig. 6d). The nighttime flow pattern was also similar to the flow pattern of 6 July (not shown). The northwestern flow over the Corinthian gulf (for its location, see Fig. 4b) seems to be channeled, and this channeling has been observed during a summer campaign performed by Asimakopoulos et al. (1994). Indeed, the authors reported that during a 1-month period (July 1993), winds were recorded at the eastern edge of the Corinthian gulf as well as at the coasts and inside the Athens Basin. It was also found that under weak synoptic flow when light winds were blowing in the Athens Basin, the winds were more intense over the Corinthian gulf. This channeling of the flow over the Corinthian gulf can be attributed to the important sloping of mountains both in the north and south of the gulf (Fig. 4b).

The stationary synoptic conditions with the weak synoptic flow also result in the development of local thermal circulations the following day, that is, 7 July 1994. It should be noted that on 7 July 1994 the divergent flow over Peloponnisos is also evident (Fig. 5c) but with a smaller vertical extent than that of the previous day. The predicted flow pattern compares well with the surface synoptic network reports. The sea-breeze cell of the Saronic Gulf (Fig. 6e) does not penetrate as far inland as during the previous day. Note that the TAT station (Fig. 3) reported a northeastern flow at noon and during the early afternoon hours, while the coastal stations GMS and ELE reported a southerly flow over the same period.

On 8 July 1994 the mesoscale flow, which developed the two previous days around Peloponnisos and enhanced the sea-breeze flow, does not develop (Fig. 5d). This can be attributed to the combination of the follow-

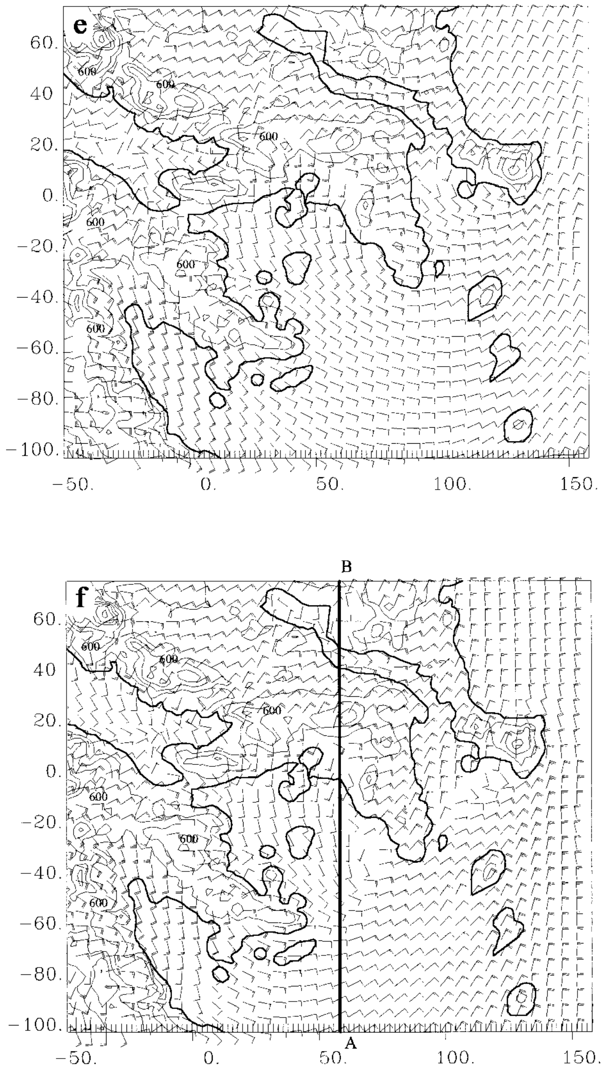

FIG. 6 (*Continued*) equals 2 m s⁻¹. Topography is plotted in 300-m intervals. Note than only a part of the inner grid is shown. Line AB in Fig. 6f shows the cross-sectional location of Figs. 8–9.

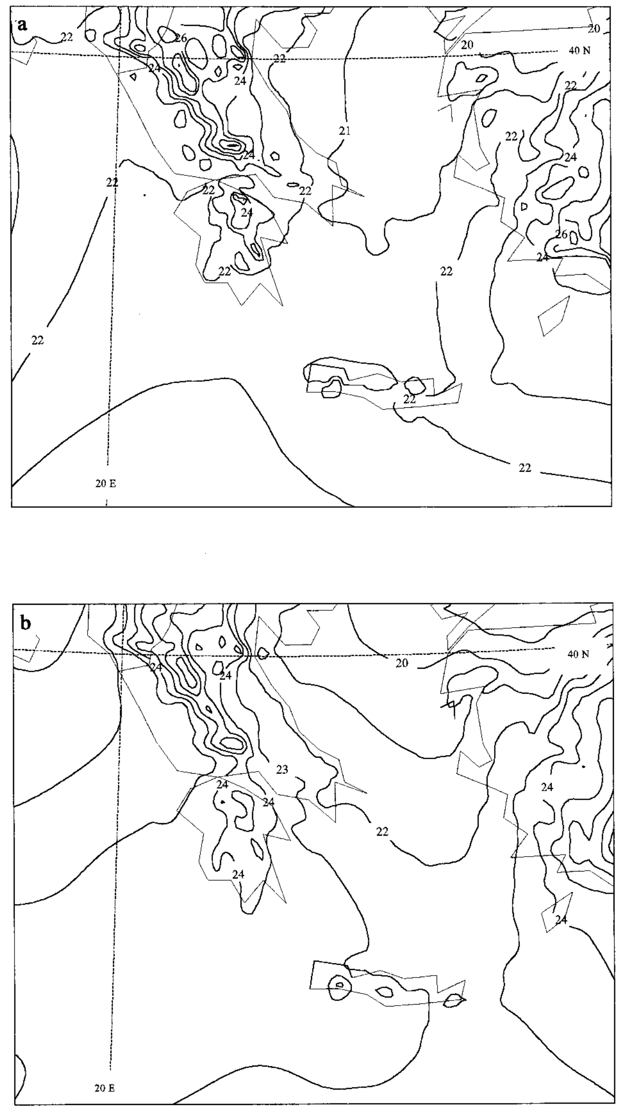

FIG. 7. Temperature at 850-hPa level (at 1°C intervals) from the second grid of RAMS at (a) 1200 UTC 6 July and (b) 1200 UTC 7 July 1994.

ing factors. The first is the reduction of vertical stability, which on the previous days forced the flow to diverge around the obstacle of Peloponnisos rather than to pass over it. The second factor is the distribution of the pressure field at the surface, which produced an intensification of the flow over the Aegean Sea (associated with a slight increase in the pressure gradient) and a weakening of the flow over the Ionian Sea (associated with a slight decrease in the pressure gradient) from 6 to 8 July. This result is supported by both the model results and the synoptic network wind and pressure reports. At 1200 UTC 8 July, the sea-breeze flow is evident over the Saronic Gulf (Fig. 6f).

As mentioned in section 2, the sounding analysis showed warm advection at the lower-tropospheric layers during the period of interest. The model successfully reproduced this warm advection at the lower-tropospheric layers from 6 to 7 July 1994. Inspection of the 850-hPa-level temperature field (Fig. 7) showed an almost 2-K warming in a 24-h interval (from 1200 UTC 6 July to 1200 UTC 7 July) over the Athens Basin. Moreover, the prevailing temperature at 850 hPa (22°–23°C) greatly exceeds the climatological value. (17°C). This climatological value was estimated in Kassomenos et al. (1995), in which the authors cited that the temperature at 850 hPa during air pollution episodes almost always exceeded the climatological value.

A further insight into the development and vertical extent of the sea breeze as well as into the boundary layer characteristics during this episode event can be assessed through the inspection of the potential tem-

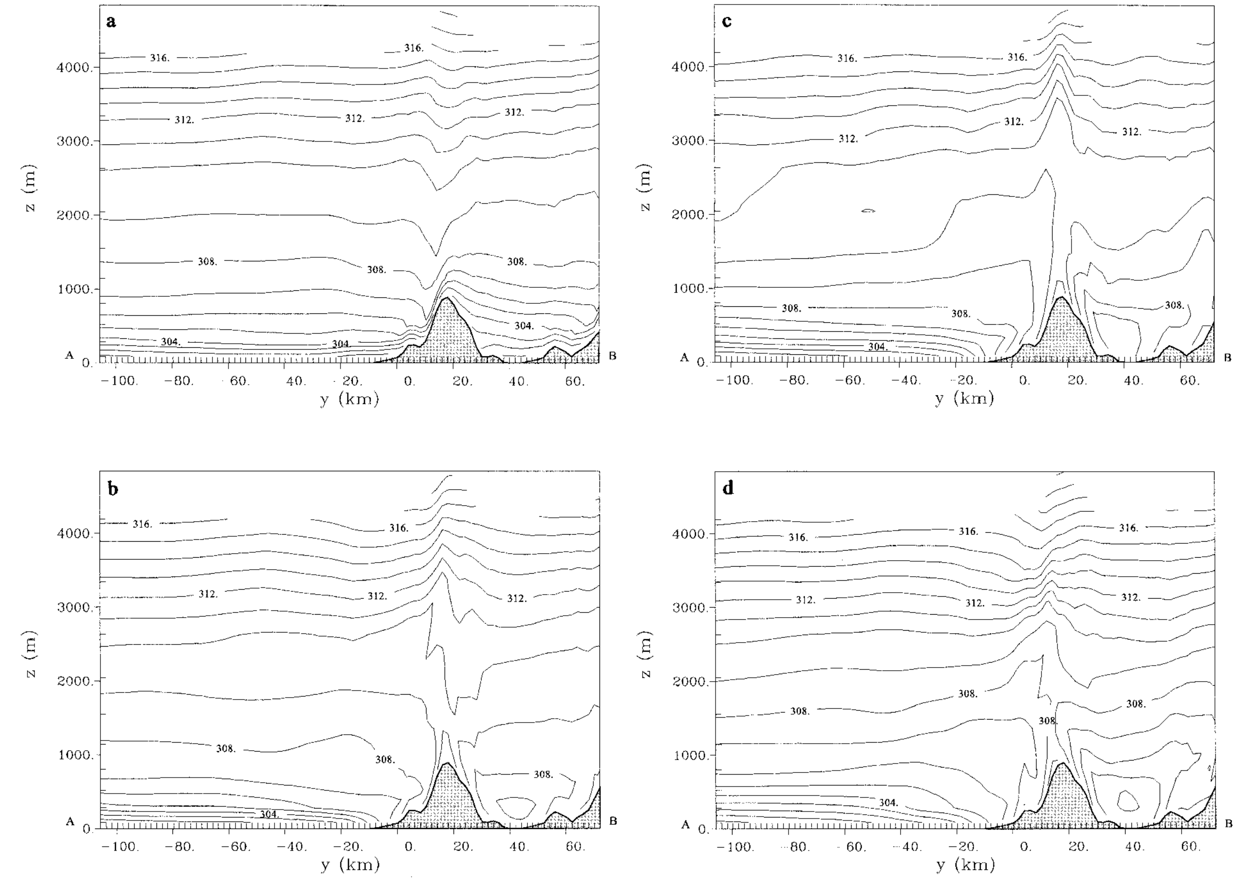

FIG. 8. North–south vertical cross section of the potential temperature field (at 1-K interval) along the 23.66°E longitude (following line AB in Fig. 7f) at (a) 0300 UTC 6 July, (b) 1200 UTC 6 July, (c) 1200 UTC 7 July, and (d) 1200 UTC 8 July 1994.

perature and wind cross sections along the Athens Basin. Figure 8 shows a set of north–south cross sections of the lower-tropospheric layers of the potential temperature field along the 23.660°E longitude from the inner grid of RAMS (following line AB in Fig. 6f). The marine boundary layer is characterized by strong stratification during both night (Fig. 8a) and day hours (Fig. 8b). At noon, vertical orientation of the isentropes over land indicates that strong convection developed onshore producing a well-mixed layer (Fig. 8b). The depth of the mixing layer is low offshore (about 300 m) and rises to approximately 600 m at the coastline. At a distance of 20 km inland the mixing depth rises sharply to 1700 m. Air temperature near the surface predicted by RAMS over the Athens Basin at 1200 UTC 6 July exceeds 34°C, which is in very good agreement with the GMS (a coastal) surface station report of 33.8°C and the NOA (a city center station report of 35.6°C. This same situation is reproduced at 1200 UTC 7 July (Fig. 8c), although the mixing depth inland is deeper than the previous day (about 2 km deep). On 8 July the mixing depth is relatively suppressed, going up to 1 km inland (Fig. 8d).

A set of vertical cross sections of the north–south wind component is given in Fig. 9. A sea breeze develops in a formerly opposing (offshore) flow. At 1200 UTC 6 July 1997 the sea breeze is fully developed (Fig. 9a). As already mentioned this flow is not a pure sea breeze but a flow resulting from the interaction of the local-scale thermal circulation with the mesoscale southerly flow over the Saronic Gulf related to the divergent flow around Peloponnisos (Fig. 5b). This mesoscale flow, which adds up with the sea breeze, shows that special care should be given when studying sea-breeze development over the Attica Peninsula. The model domain definition seems very important when this type of interaction between the regional and local scale is to be studied (Kallos and Kassomenos 1994; Kallos et al. 1993). As the topographic features on a larger scale play an important role in the definition of the atmospheric flow over the GAA, the model grid should at least include the Greek peninsula with the North African coast to the south, the Ionian and Adriatic Seas to the west, and the Aegean Sea with the western coast of Turkey to the east. A simulation with a horizontal grid increment of 2–3 km with a domain covering this large area would require computer resources that are not easily

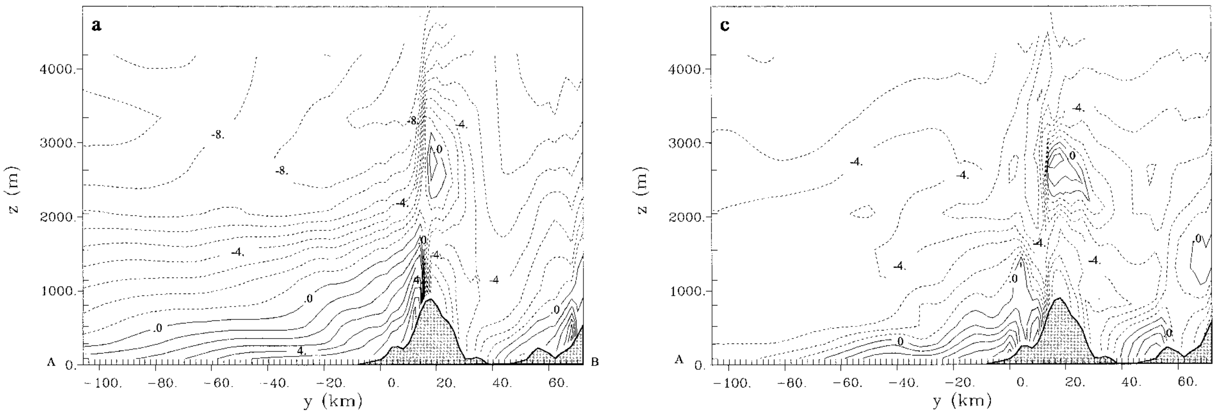

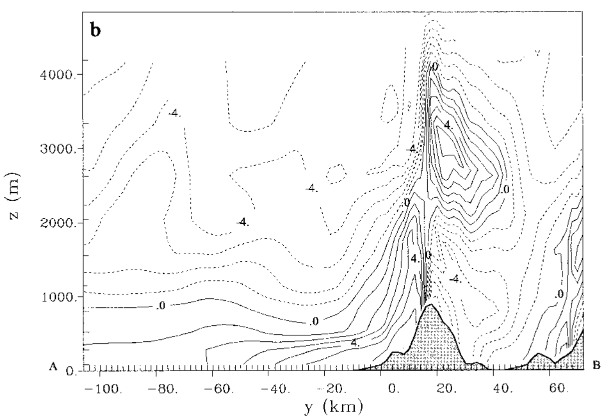

FIG. 9. North–south vertical cross section of the north–south wind component field (in 1 m s^{-1} intervals) along the 23.660°E longitude (following line AB in Fig. 7f) at (a) 1200 UTC 6 July, (b) 1200 UTC 7 July, and (c) 1200 UTC 8 July 1994. Negative values (northern winds) are dashed.

available. Thus, a nested grid simulation is necessary in order to take into account the type of scale interaction in the area. In this case the inner grid should at least include, in addition to the Athens Basin, Evvoia Island in the east, the northeastern coast of Peloponnisos, and the Corinthian gulf. In Figure 9a, an offshore flow is evident above 1000-m height at the coastline and at about 1700 m farther inland, but it is difficult to conclude which part of it is due to the return flow of the sea breeze. Similar characteristics are evident in the 7 July cross section (Fig. 9b), but it should be noted that the southerly flow is weaker over the Athens Basin than during the previous day. At 1200 UTC 8 July, the sea-breeze flow is shallow (up to 400–500 m deep near the coastline, reaching a depth of 800–1000 m inland) and of weaker intensity (Fig. 9c). Note that, as already discussed, during this day there is no southerly mesoscale flow that enhanced the southerly sea-breeze flow the previous two days. This is evident in Fig. 9c where the southerly flow (positive values) starts 50 km offshore to the south, while during the previous days it was evident offshore to the south up to the southern edge of the domain (Figs. 9a,b).

b. Dispersion results compared to air quality observations

The development of local thermal circulations plays a very important role in pollutant dispersion since it results in a complex wind field. In order to have an insight into the path that urban air follows and the impact that the urban plume could have on remote locations, dispersion simulations were performed using the HYPACT model.

More precisely, a simulation was performed using the Lagrangian option of HYPACT in which a rectangular source of pollutants was specified over the greater Athens area. One single particle was released every 30 s from a 10 km × 10 km × 0.2 km grid volume located over the GAA, which represents the multiple sources in the area. The aim of the simulation was to track the path of the urban plume during an air pollution episode. Moreover, using the ‘‘age’’ of the emitted particles, it was possible to investigate the role of transport and recirculation processes. The particle release started at 0000 UTC 6 July 1994 and was continuous for 72 h. In all subsequent figures, only particles confined within the first 1000 m will be shown.

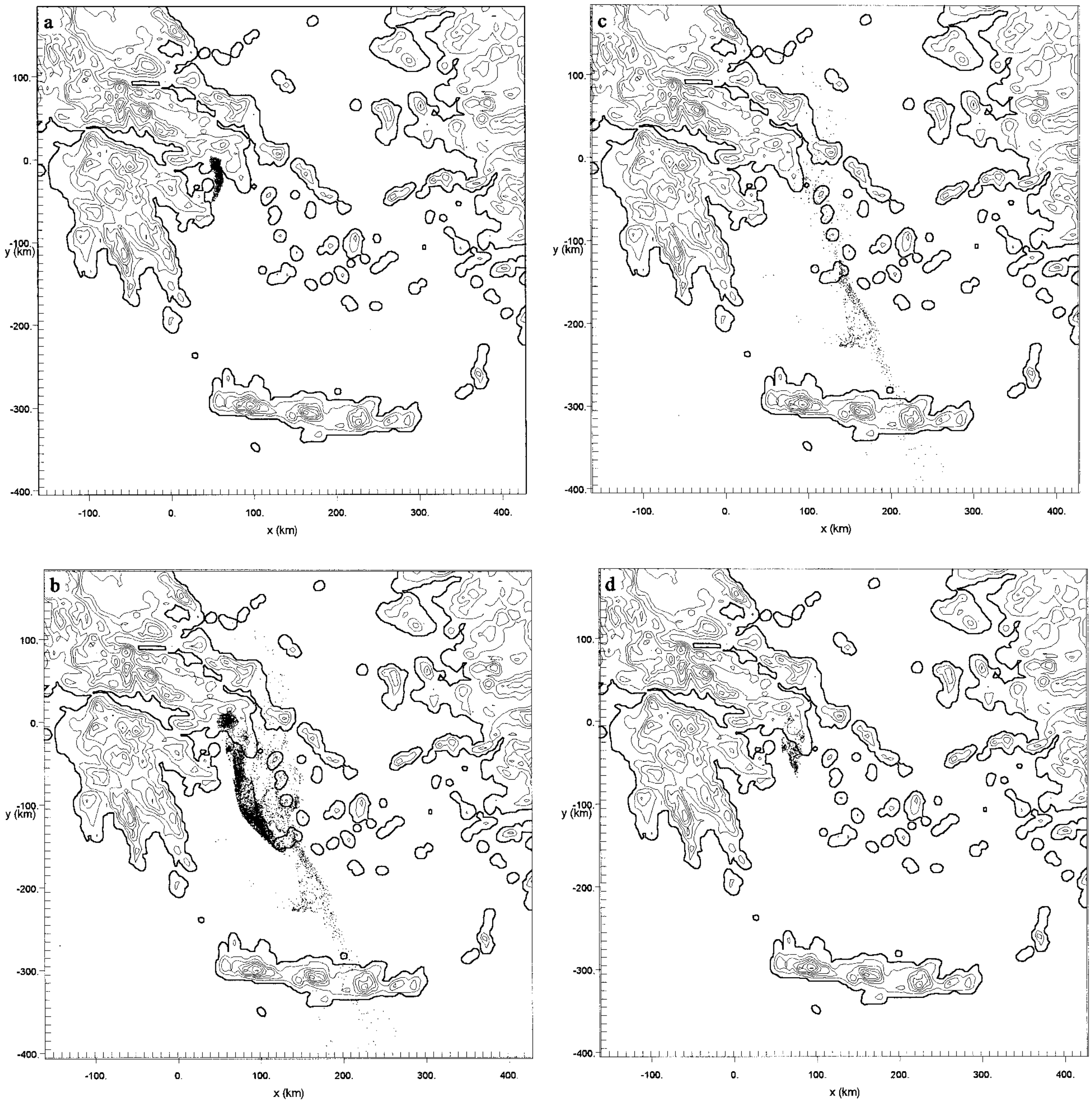

FIG. 10. Particles in the layer 0–1000 m from the HYPACT dispersion model at (a) 1200 UTC 6 July, after 9 h of particle release; (b) 0900 UTC 7 July, after 30 h of particle release; (c) as in (b) but only the particles emitted from 0300 to 0900 UTC 6 July are plotted; and (d) as in (b) but only the particles emitted from 0300 to 0600 UTC 7 July are plotted. (e) At 1300 UTC 7 July, after 34 h of particle release;

From 0800 to 1500 UTC 6 July 1994 high surface ozone concentrations exceeding 80 ppbv with peaks of 120 ppbv were reported from the surface air quality monitoring network (see also Peleg et al. 1997). At 1200 UTC 6 July dispersion results showed that polluted air masses were advected from the Athens Basin over the Saronic Gulf and east of Aegina Island (Fig. 10a), showing that the urban plume can affect areas downwind from Athens within a short time interval (5–6 h) after their release.

The following day, at 0900 UTC 7 July, the polluted air masses within the first kilometer are found over the eastern Saronic Gulf and farther south at approximately 150 km from Athens (Fig. 10b), while at higher altitudes they are found within a belt oriented north–south from the central Aegean Sea to southern Crete (not shown). The flight performed during the morning hours on 7 July (Fig. 11a) supports these results with low ozone concentrations (below 60 ppbv) in the maritime area east of Peloponnisos, high concentration over the Athens Basin, and a secondary maximum over the eastern

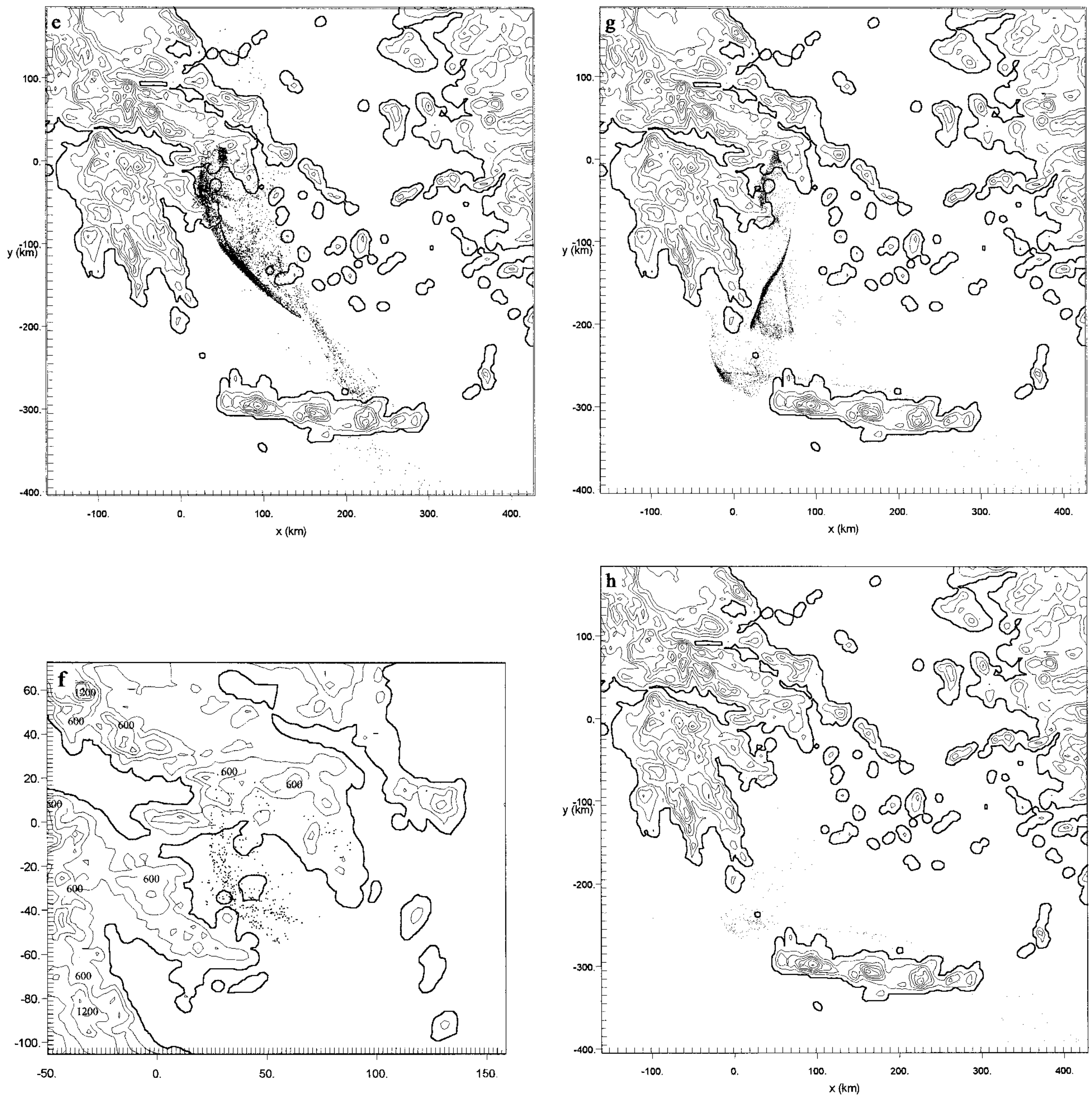

FIG. 10 (*Continued*) (f) as in (e) but only the particles emitted from 0300 to 0600 UTC 7 July are plotted in the same domain as in Fig. 6; topography is plotted every 300 m; (g) 1000 UTC 8 July, after 55 h of particle release; and (h) same as in (g) but only the particles emitted from 1200 to 1800 UTC 6 July are plotted; and (i) same as in (g) but only the particles emitted from 1200 to 1800 UTC 7 July are plotted.

Saronic Gulf. At this point it would be helpful to discuss the age of the particles in this plume. Figure 10c shows the position of the particles at 0900 UTC 7 July that were emitted during the previous day (from 0300 to 0900 UTC 6 July 1994). Comparison with Fig. 10b shows that particles emitted during the previous day do not affect the concentrations on 7 July over the Athens Basin, as they have been advected eastward by the nocturnal western flow over the Corinthian and Saronic Gulfs depicted in Fig. 6d and then advected southward by the northerly flow prevailing over the Aegean Sea. Figure 10d shows the position of the particles emitted during the same day (from 0300 to 0600 UTC 7 July 1994) at 0900 UTC 7 July. It is obvious that the dense plume over the eastern Saronic Gulf depicted in Fig. 10b is mainly formed by particles emitted during the early morning hours of 7 July.

Figure 10e shows the position of particles emitted continuously until 1300 UTC 7 July 1994. Dispersion results show high particle concentrations over the Ath-

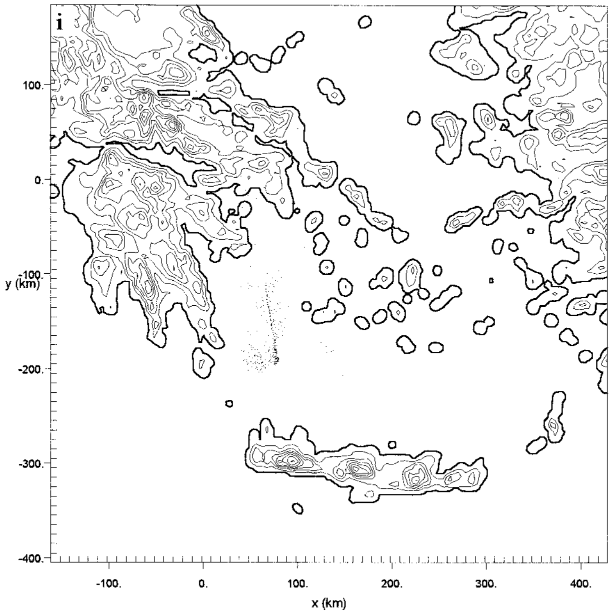

FIG. 10 (*Continued*)

ens Basin as well as over the entire Saronic Gulf and near the northeastern coasts of Peloponnisos. The research aircraft performed the second experimental flight of the day over Athens and the Saronic Gulf from 1140 to 1430 UTC 7 July (Fig. 11b). Note that concentrations of the order of 100–120 ppbv were measured over the GAA, and of the order of 80–100 ppbv over the western and central Saronic Gulf (where the model-predicted plume is dense), while farther to the east the measured concentrations were of the order of 60–80 ppbv (where the particle plume is substantially less dense). Following again the particles emitted during the morning of the same day (from 0300 to 0600 UTC 7 July 1994) we can see (Fig. 10f; note that this figure shows the position of particles inside a domain coinciding with the inner grid of RAMS) that these particles, which were initially advected over the eastern Saronic Gulf during the morning (see Fig. 10c), have been advected northwestward by the wind flow and at 1300 UTC 7 July are found mainly along the northeastern coast of Peloponnisos and over and south of Aegina Island. Following these particles later during 7 July (not shown), it can be concluded that they are not advected very far from the Athens Basin but instead stay confined over the Saronic Gulf and northeastern Peloponnisos.

Figure 10g shows the position of particles emitted continuously until 1000 UTC 8 July 1994. High particle concentrations are found following an axis from Athens to western Crete, with the highest concentrations over the Athens Basin, as well as over the maritime area between Peloponnisos and Crete. The research aircraft performed an experimental flight during this day, following a path southward along the Peloponnisos coast down to western Crete (Fig. 11c). The airborne observations support the dispersion results, in the sense that measured ozone concentrations (higher than 60 ppbv) along the flight path exceed the background concentrations, and a peak of ozone exceeding 80 ppbv offshore southeastern Peloponnisos was reported (consistent with the predicted dense plume in the area). Inspection of the SO_2 measured concentrations during the same flight showed also a peak in the same area (not shown). As the residence time of SO_2 permits the use of this pollutant as a tracer, for the timescales considered in this case, and as there are no local sources that could have contributed to the measured concentrations, it can be concluded that the air masses in the area of southeastern Peloponnisos have been advected there. These indications along with the dispersion results imply that the urban plume of Athens can affect areas located 150–200 km away from the GAA. The high particle concentrations east of Crete, depicted in Fig. 10g, have been emitted during the afternoon hours of 6 July 1994 (1200–1800 UTC). These particles were initially advected east of the Athens Basin toward the central Aegean Sea. On 7 July these particles were advected over the maritime area east of Peloponnisos, where the existence of the weak southerly flow depicted in Fig. 5c prohibited their further progression southward. During the night and early morning of 8 July the prevailing northeastern flow advects the particles east of Crete (Fig. 10h). On the other hand, an important part of the plume, depicted in Fig. 10g, over the maritime area east of Peloponnisos consists of particles emitted during the day hours (from 1200 to 1800 UTC) of 7 July (Fig. 10i).

5. Concluding remarks

In this study the meteorological conditions prevailing during an air pollution episode were analyzed based on the available observations and model results. The accurate reproduction of the atmospheric circulations is essential to air pollution control studies, as the predicted meteorological fields can have a greater impact on photochemical models than the chemical mechanisms represented in these models. This study demonstrates that one should look well beyond the local scale in order to understand the prevailing atmospheric flow and dispersion characteristics within the GAA. The model domain should at least include the Greek peninsula with the North African coast to the south, the Ionian and Adriatic Seas to the west, and the Aegean Sea with the western coast of Turkey to the east. A fine resolution (2–3-km horizontal grid increment) covering this large area would require computer resources that are not easily available. Thus, it is fundamental to perform a nested grid simulation in order to take into account the interaction of the different scales of motion in defining the local-scale flow. Farther the inner grid should include, in addition to the GAA, the island of Evvoia to the east, the Corinthian gulf to the west, and the eastern coast of Peloponnisos. Indeed, the nesting capabilities of RAMS

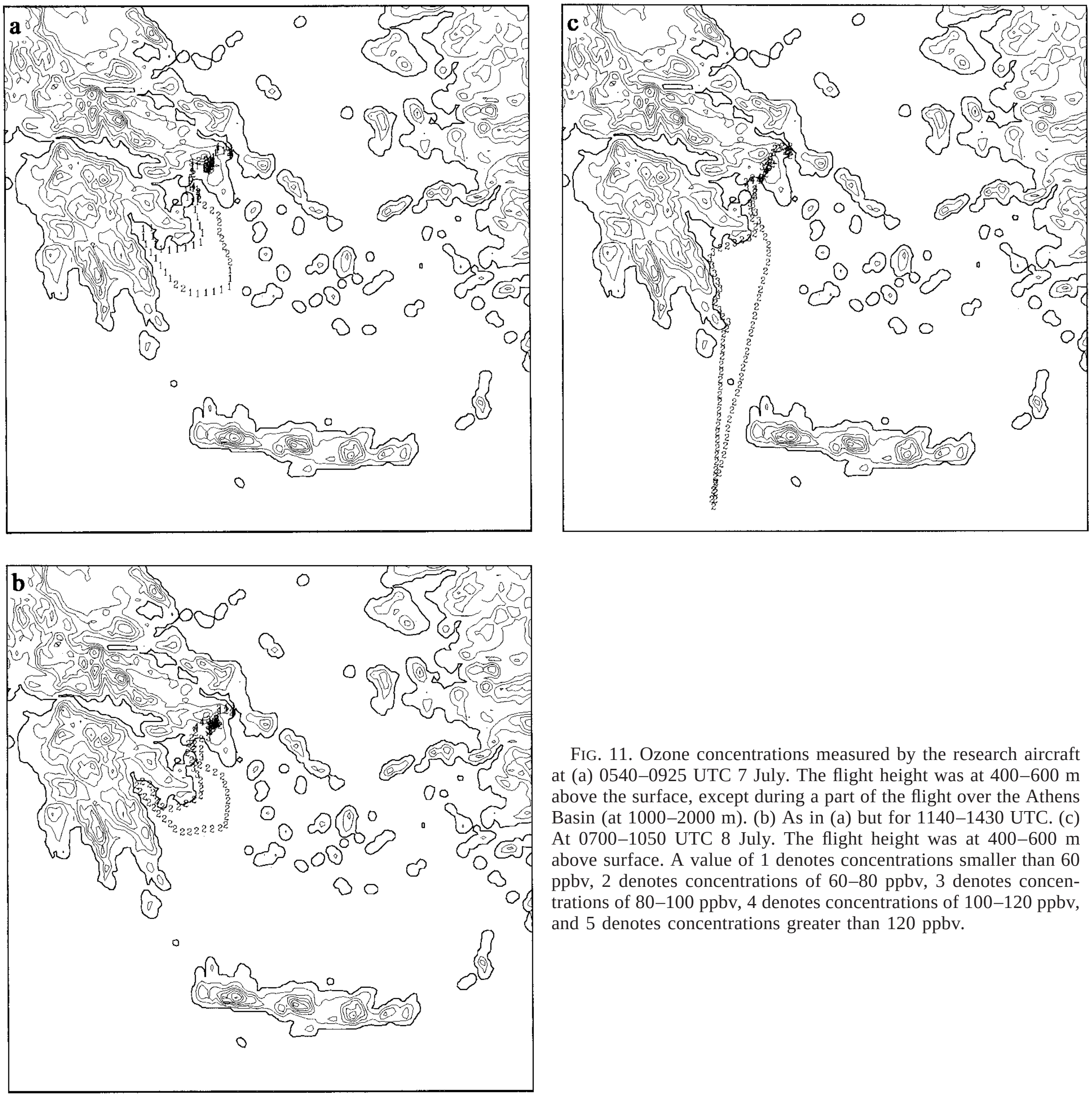

FIG. 11. Ozone concentrations measured by the research aircraft at (a) 0540–0925 UTC 7 July. The flight height was at 400–600 m above the surface, except during a part of the flight over the Athens Basin (at 1000–2000 m). (b) As in (a) but for 1140–1430 UTC. (c) At 0700–1050 UTC 8 July. The flight height was at 400–600 m above surface. A value of 1 denotes concentrations smaller than 60 ppbv, 2 denotes concentrations of 60–80 ppbv, 3 denotes concentrations of 80–100 ppbv, 4 denotes concentrations of 100–120 ppbv, and 5 denotes concentrations greater than 120 ppbv.

successfully reproduced the observed flow pattern during the air pollution episode event of 6–8 July 1994, mainly the channeling of flow over the Corinthian gulf, the divergent flow around Peloponnisos, as well as the development of sea-breeze cells over the GAA.

The sea-breeze cell development on 6 and 7 July was produced by the interaction of the local-scale thermal circulation with the southern mesoscale divergent flow around Peloponnisos. This predicted flow was in good agreement with the observations provided by the surface synoptic network. The divergence of the flow around Peloponnisos can be expected under a weak synoptic flow and when warm air advection in the lower-tropospheric layers produces a stabilization of the lower-tropospheric flow. On 8 July, this southerly mesoscale flow does not develop due to the reduction of vertical stability and due to the distribution of the pressure field at the surface, which produced an intensification of the flow over the Aegean Sea and a weakening of the flow over the Ionian Sea. The interaction of the local scale with the mesoscale evidenced during this event shows that special care should be given when studying sea-breeze development over the Attica Peninsula. Moreover, RAMS also reproduces the warm advection at the 850 hPa, which is a critical mechanism during air pollution episodes.

The influence of the urban plume on the air quality of remote locations has been studied through simulations with the HYPACT model. Based on a 72-h Lagrangian simulation (from 0000 UTC 6 July to 0000 UTC 9 July 1994), the path of the emitted particles from the Athens Basin during this event is studied. The model results showed that for that particular air pollution episode

1) there is no recirculation of air pollutants over the Athens Basin;
2) particles influence the air quality over the Saronic Gulf within 5–6 h from the time of emission; and
3) particles can travel a long distance over the maritime areas of the Saronic Gulf and the western Aegean Sea, influencing the air quality over areas as far as 200 km to the south of the GAA on a timescale of the order of 36 h.

These results compare favorably with the concentrations measured by the research aircraft during the same period, which measured high concentrations (e.g., O_3, exceeding 80 ppbv) along the southeastern coast of Peloponnisos, as well as concentrations higher than the background concentrations (e.g., O_3 of the order 60–80 ppbv) in the maritime area between Peloponnisos and Crete.

Acknowledgments. The authors thank Dr. C. Tremback (ASTER Division of the Mission Research Corporation) for his helpful comments. This research was partially supported by the AVICENNE Initiative, Contract EV*-CT92-0005 of the DG-XII of the EU, and by the Ministry of the Environment, City Planning and Public Works (Program ETERPS). Acknowledgment is made to the National Center for Atmospheric Research, which is sponsored by the National Science Foundation, for some of the computing time used in this research and for providing the sounding and surface data used in this study (Contract 35081147).

REFERENCES

Asimakopoulos, D. N., D. Deligiorgi, C. Drakopoulos, C. Helmis, K. Kokkori, D. P. Lalas, D. Sikiotis, and C. Varotsos, 1992: An experimental study of nighttime air pollutant transport over complex terrain in Athens. *Atmos. Environ.,* **26B,** 59–71.

——, C. G. Hemis, M. Petrakis, and M. Tombrou, 1993: Atmospheric boundary layer field measurements over coastal areas. *Environ. Software,* **8,** 9–18.

——, ——, G. Kallos, J. Kalogiros, K. H. Papadopoulos, M. Petrakis, and A. T. Soilemes, 1994: The SECAP experimental campaign during summer 1993. Intermediate Report prepared for the DGXII of the EU, 150 pp. [Available from Laboratory of Meteorology, University of Athens, PHYS-5, Athens 15784, Greece.]

Bossert, J. E., 1997: An investigation of flow regimes affecting the Mexico City region. *J. Appl. Meteor.,* **36,** 119–140.

Fast, J. D., B. L. O'Steen, and R. P. Addis, 1995: Advanced atmospheric modeling for emergency response. *J. Appl. Meteor.,* **34,** 626–649.

Giovannoni, J.-M., and A. Russell, 1995: Impact of using the prognostic and objective wind fields on the photochemical modelling of Athens, Greece. *Atmos. Environ.,* **29B,** 3633–3654.

Helmis, C. G., D. N. Asimakopoulos, D. G. Deligiorgi, and D. P. Lalas, 1987: Observations of sea breeze fronts near the shoreline. *Bound.-Layer Meteor.,* **38,** 395–410.

——, K. H. Papadopoulos, J. A. Kalogiros, A. T. Soilemes, and D. A. Asimakopoulos, 1995: Influence of background flow on evolution of Saronic Gulf sea breeze. *Atmos. Environ.,* **29B,** 3689–3701.

Kallos, G., and P. Kassomenos, 1994: Effects of the selected domain in mesoscale atmospheric simulations and dispersion calculations. *Proceedings of the 20th ITM of NATO/CCMS on Air Pollution Modeling and Its Application,* S. Gryning and M. Millan, Eds., Plenum, 35–44.

——, ——, and R. A. Pielke, 1993: Synoptic and mesoscale weather conditions during air pollution episodes in Athens, Greece. *Bound.-Layer Meteor.,* **62,** 163–184.

——, and Coauthors, 1996: Transport and transformation of air pollutants from Europe to the East Mediterranean. Final Rep. for the DGXII of EU, Environmental Research Program AVICENNE, 352 pp. [Available from Laboratory of Meteorology, University of Athens, PHYS-5, Athens 15784, Greece.]

Kassomenos, P., V. Kotroni, and G. Kallos, 1995: Analysis of the climatological and air quality observations from the greater Athens area. *Atmos. Environ.,* **29B,** 3671–3688.

Kunz, R., and N. Moussiopoulos, 1995: Simulation of the wind field in Athens using refined boundary conditions. *Atmos. Environ.,* **29B,** 3575–3592.

Lagouvardos, K., V. Kotroni, and G. Kallos, 1996: Exploring the effects of different types of model initialisation: Simulation of a severe air-pollution episode in Athens, Greece. *Meteor. Appl.,* **3,** 147–155.

Lalas, D. P., V. R. Veirs, G. Karras, and G. Kallos, 1982: An analysis of the SO_2 concentration levels in Athens, Greece. *Atmos. Environ.,* **16,** 531–544.

——, D. Asimakopoulos, D. Deligiorgi, and C. Helmis, 1983: See breeze circulation and photochemical pollution in Athens, Greece. *Atmos. Environ.,* **17,** 1621–1631.

——, M. Tombrou-Tsella, M. Petrakis, D. N. Asimakopoulos, and C. G. Helmis, 1987: An experimental study of the vertical distribution of ozone over Athens. *Atmos. Environ.,* **12,** 2681–2693.

Lyons, W. A., R. A. Pielke, W. R. Cotton, M. Uliasz, C. J. Tremback, R. L. Walko, and J. L. Eastman, 1993: The applications of new technologies to modelling mesoscale dispersion in coastal zones and complex terrain. *Air Pollution,* P. Zannetti, C. A. Brebbia, J. E. Carcia Gardea, and G. A. Milian, Eds., Elsevier, 35–85.

——, ——, ——, C. J. Tremback, R. L. Walko, M. Uliasz, and J. I. Ibarra, 1994: Recent applications of the RAMS meteorological and the HYPACT dispersion models. *Proceedings of the 20th ITM of NATO/CCMS on Air Pollution Modeling and Its Application,* S. Gryning and M. Millan, Eds., Plenum, 19–26.

——, C. J. Tremback, and R. A. Pielke, 1995: Applications of the Regional Atmospheric Modeling System (RAMS) to provide input to photochemical grid models for the Lake Michigan Ozone Study (LMOS). *J. Appl. Meteor.,* **34,** 1762–1786.

Melas, D., I. Ziomas, and C. Zerefos, 1995: Boundary layer dynamics in an urban coastal environment under sea breeze conditions. *Atmos. Environ.,* **29B,** 3605–3618.

Peleg, M., M. Luria, G. Sharf, A. Vanger, G. Kallos, V. Kotroni, K. Lagouvardos, and M. Varinou, 1997: Observational evidence of an ozone episode over the greater Athens area. *Atmos. Environ.,* **31,** 3969–3983.

Pielke, R. A., W. A. Lyons, R. T. McNider, M. D. Moran, R. A. Stocker, R. L. Walko, and M. Uliasz, 1991: Regional and mesoscale meteorological modeling as applied to air-quality studies. *Air Pollution Modeling and Its Applications VIII,* H. van Dop and D. G. Steyn, Eds., Plenum, 259–290.

——, and Coauthors, 1992: A comprehensive meteorological modeling system—RAMS. *Meteor. Atmos. Phys.,* **49,** 69–91.

Pilinis, C., P. Kassomenos, and G. Kallos, 1993: Modeling of the photochemical pollution in Athens, Greece: Application of the RAMS–CALGRID modeling system. *Atmos. Environ.,* **27B,** 353–370.

Poulos, G. S., and J. E. Bossert, 1995: An observational and prognostic numerical investigation of complex terrain dispersion. *J. Appl. Meteor.,* **34,** 650–669.

Prezerakos, N., 1986: Characteristics of the sea breeze in Attica, Greece. *Bound.-Layer Meteor.,* **32,** 245–266.

Steyn, D. G., and G. Kallos, 1992: A study of the dynamics of hodograph rotation in the sea breezes of Attica, Greece. *Bound.-Layer Meteor.,* **58,** 215–228.

Tremback, C. J., W. A. Lyons, W. P. Thorson, and R. L. Walko, 1994: An emergency response and local weather forecasting software system. *Proceedings of the 20th ITM of NATO/CCMS on Air Pollution Modeling and Its Application,* S. Gryning and M. Millan, Eds., Plenum, 423–429.

Varvayanni, M., J. Bartzis, C. Helmis, and D. N. Asimakopoulos, 1993: Simulation of the sea breeze under opposing synoptic conditions. *Environ. Software,* **8,** 19–27.